NASA TECHNICAL NOTE

NASA TN D-4073

NASA TN D-4073

STRUCTURAL EFFICIENCY OF RING-STIFFENED CORRUGATED CYLINDERS IN AXIAL COMPRESSION

by James P. Peterson

Langley Research Center

Langley Station, Hampton, Va.

NATIONAL AERONAUTICS AND SPACE ADMINISTRATION • WASHINGTON, D. C. • AUGUST 1967

NASA TN D-4073

STRUCTURAL EFFICIENCY OF RING-STIFFENED CORRUGATED CYLINDERS IN AXIAL COMPRESSION

By James P. Peterson

Langley Research Center
Langley Station, Hampton, Va.

NATIONAL AERONAUTICS AND SPACE ADMINISTRATION

For sale by the Clearinghouse for Federal Scientific and Technical Information
Springfield, Virginia 22151 – CFSTI price $3.00

STRUCTURAL EFFICIENCY OF RING-STIFFENED CORRUGATED CYLINDERS IN AXIAL COMPRESSION

By James P. Peterson
Langley Research Center

SUMMARY

Results of an analytical study of desirable proportions of corrugated ring-stiffened cylinders are presented. The corrugated walls of the cylinders studied consisted of narrow, equal thickness, flat elements joined along longitudinal edges. The rings could have any of a wide range of cross-sectional geometries and could be fastened to either the inside or the outside surface of the cylinder wall. The study indicates that the corrugated wall should be constructed of elements which have width-thickness ratios as large as possible without introducing local buckling of the elements; the wall should be formed with angles between adjacent elements of approximately 120° ($\phi = 60^{\circ}$).

The study of cylinders with internal stiffening indicates that unsymmetrical rings (T-section) are preferable to symmetrical rings (I-section), and that the rings should have a mass of approximately 30 percent of that of the corrugated wall. Moreover, the rings should normally be spaced as far apart as possible without introducing wall failure between rings. Little advantage, if any, is found in substituting magnesium rings for aluminum rings on an aluminum cylinder, in substituting closed hat-section rings for T-section rings, or in substituting rings with webs having lightening holes for rings with solid webs.

For externally stiffened cylinders, ring shape and ring spacing are found to be relatively unimportant, but ring area is again important; rings with a mass of 1/3 of that of the corrugated wall are found to lead to stiffened cylinders with the lowest mass-strength ratios.

The corrugated cylinders are compared with honeycomb sandwich cylinders on a mass-strength basis. The corrugated cylinders with external stiffening are found to be more attractive than the honeycomb sandwich cylinders on this basis and the cylinders with internal stiffening are found to be somewhat less attractive.

INTRODUCTION

The ring-stiffened corrugated cylinder is an attractive structure from a low-mass, high-strength point of view for the intertank and interstage sections of large launch vehicles (ref. 1). Accurate design of corrugated cylinders to withstand compressive in-plane stresses requires the use of buckling equations which take into account the eccentricity (one-sidedness) of the stiffening rings. For cylinders with internal stiffening, such equations indicate that, on the one hand, deep rings are attractive because deep rings provide large moments of inertia which enhance the buckling characteristics of the cylinder; while, on the other hand, shallow rings are attractive because shallow rings keep ring eccentricity small and hence also enhance the buckling characteristics of the cylinders. Thus, it would appear that an optimum-depth ring is associated with each design situation, and that the depth is a compromise between the "forces" of moment of inertia and those of ring eccentricity.

The purpose of the present paper is to determine desirable ring and corrugation properties for cylinders having low-mass, high-strength characteristics and to compare the structural efficiency of such cylinders with that obtained in a previous study for honeycomb sandwich cylinders. Both internally stiffened and externally stiffened corrugated cylinders are considered. The general theory which applies to either inside or outside stiffening is presented first; then cylinders with internal stiffening are considere and finally cylinders with outside stiffening are considered.

SYMBOLS

The units used for the physical quantities in this paper are given both in the U.S. Customary Units and in the International System of Units (SI) (ref. 2). Factors relating the two systems of units for quantities used in the present investigation are given in the appendix.

A	cross-sectional area of column
A_F	cross-sectional area of flanges of stiffening ring (see fig. 1(b))
A_r	cross-sectional area of stiffening ring, $A_F + A_W$
A_W	cross-sectional area of web of stiffening ring (see fig. 1(b))
A_1, A_2, A_3	defined after equation (3)

b width of flat plate element of corrugation (see fig. 1(a))

d density of corrugation material

d_r density of ring material

D_x, D_y bending stiffness of corrugated cylinder wall in axial direction and circumferential direction, respectively

D_{xy} twisting stiffness of corrugated cylinder wall

E Young's modulus of corrugation material

E_r Young's modulus of ring material

E_s secant modulus of corrugation material

E_t tangent modulus of corrugation material

E_x, E_y extensional stiffness of corrugated cylinder wall in axial direction and circumferential direction, respectively

f depth of corrugation (see fig. 1(a))

F_S shape factor

G_r shear modulus of ring material

G_{xy} in-plane shear stiffness of corrugated cylinder wall

h depth of ring (see fig. 1(b))

I_r moment of inertia of ring about its centroid

J_r torsional constant of ring

k ratio of area of flange material in attached flange to total flange area of stiffening ring (see fig. 1(b))

l ring spacing

n number of full waves in buckle pattern in circumferential direction of cylinder

N_x load per unit length of cylinder circumference at buckling

R radius of cylinder measured to middle surface of corrugated wall

t sheet thickness of material of corrugated wall of cylinder (see fig. 1(a))

t_W thickness of web of stiffening ring (see fig. 1(b))

$\bar{t}$ equivalent wall thickness of corrugated cylinder wall and rings, $\bar{t}_x + \frac{d_r}{d}\frac{A_r}{l}$

$\bar{t}_x$ equivalent thickness of corrugated wall of cylinder

$\bar{y}$ distance from centroid of stiffening ring to attachment between stiffening ring and corrugated wall (see fig. 1(b))

$\bar{z}_r$ distance from centroid of stiffening ring to middle surface of corrugated wall (see fig. 1(b)), negative distance for cylinder with inside rings

β buckle aspect ratio, ratio of wavelength of buckles in axial direction to wavelength in circumferential direction

γ ratio of material in flanges of stiffening ring to total material in ring, A_F/A_r

δ ratio of density of core of honeycomb sandwich cylinder to density of face sheets of sandwich

ϵ strain at buckling

μ Poisson's ratio of corrugation material

μ_x, μ_y Poisson's ratio associated with bending of corrugated wall of cylinder in axial direction and circumferential direction, respectively

μ_x', μ_y' Poisson's ratio associated with extension of corrugated wall of cylinder in axial direction and circumferential direction, respectively

ρ radius of gyration of column

$\rho_r = \sqrt{\frac{I_r}{A_r}}$

σ stress at buckling

ϕ corrugation angle (see fig. 1(a))

Subscripts:

Al aluminum

corr corrected

gen general-instability buckling

loc local buckling of elements of corrugated wall

pan panel-instability buckling

Mg magnesium

THEORY

Approximate buckling equations are often used in structural efficiency studies for convenience; their use is normally adequate for predicting trends and desirable structural proportions and shapes. The equations used in the present study are considered only fair for predicting the buckling loads of ring-stiffened corrugated cylinders and a discussion of the influence of the equations on the results of the investigation is given in a subsequent section of the paper.

The wall and ring sections of the cylinder studied are shown in figure 1. Rings are attached to either the inside or the outside surface of the cylinder and the cylinder is presumed to be long enough to accommodate several buckles. The contribution of the

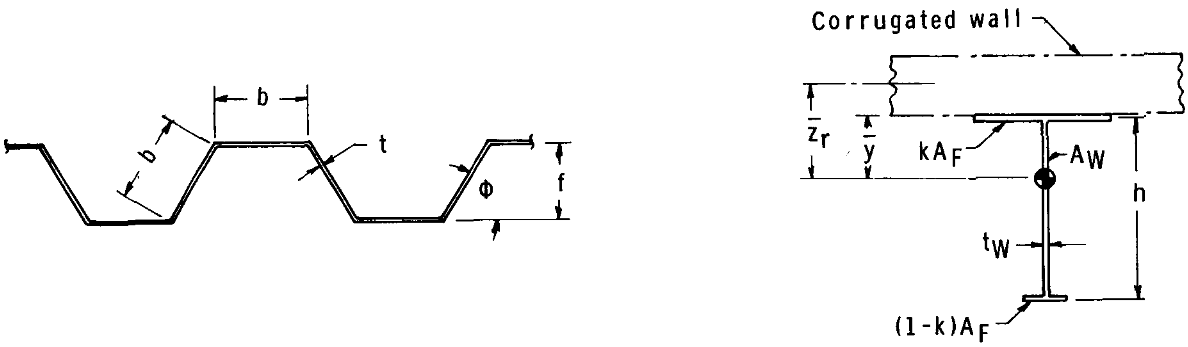

(a) Corrugated wall.

(b) Stiffening ring.

Figure 1.- Nomenclature associated with cylinder dimensions.

rings in supporting the corrugated wall is assumed to be "smeared out" over the ring spacing. Use of these assumptions considerably simplifed buckling equations. Buckling equations can be further simplified by neglecting certain stiffnesses which introduce only small errors in the calculated buckling load. Hence the following assumption is made in the calculations of this report in assigning properties to the corrugated wall:

$$\left.\begin{aligned} \mu_x = \mu_y = \mu_x{}' = \mu_y{}' = 0 \\ D_y = D_{xy} = E_y = 0 \end{aligned}\right\} \tag{1}$$

The buckling load of ring-stiffened corrugated cylinders is given by equation (15) of reference 3. With the use of equations (1), the reference equation can be written as

$$\frac{N_x R^2}{D_x} = \frac{n^2}{\beta^2}\left(1 + \frac{G_r J_r}{D_x l}\beta^2 + \frac{E_r I_r}{D_x l}\beta^4\right) + R^2 \frac{E_r A_r}{D_x l}\frac{\beta^2}{n^2}\frac{\left(1 + \frac{\bar{z}_r}{R} n^2\right)^2}{1 + \frac{E_r A_r}{G_{xy} l}\beta^2 + \frac{E_r A_r}{E_x l}\beta^4} \tag{2}$$

for an axially loaded corrugated cylinder without axial stiffening. A further reduction in the number of parameters entailed in buckling calculations can be obtained by minimizing equation (2) with respect to the number of circumferential waves n. This procedure results in the following buckling equation which must be minimized with respect to the buckle aspect ratio β in order to determine the buckling load N_x:

$$\frac{N_x R}{\sqrt{D_x \frac{E_r A_r}{l}}} = \frac{2}{A_2}\left(\sqrt{A_1 A_2 + A_3^{\,2}} + A_3\right) \tag{3}$$

where

$$A_1 = 1 + \frac{G_r J_r}{D_x l}\beta^2 + \frac{E_r I_r}{D_x l}\beta^4$$

$$A_2 = 1 + \frac{E_r A_r}{G_{xy} l}\beta^2 + \frac{E_r A_r}{E_x l}\beta^4$$

$$A_3 = \frac{\bar{z}_r}{\rho_r}\sqrt{\frac{E_r I_r}{D_x l}}\,\beta^2$$

and

$$\rho_r = \sqrt{\frac{I_r}{A_r}}$$

Pertinent stiffnesses of corrugated sheet are given by (ref. 4)

$$\left.\begin{aligned}
E_x &= \frac{2E_t t}{1 + \cos\phi} \\
G_{xy} &= \frac{E_s t(1 + \cos\phi)}{4(1 + \mu)} \\
D_x &= \frac{E_t t b^2}{3}(1 - \cos\phi)
\end{aligned}\right\} \tag{4}$$

where the secant and tangent moduli are used in place of Young's modulus in order to approximate the behavior of corrugated sheet at stresses both above and below the proportional limit of the sheet material.

An equation suitable for calculating low-mass, high-strength cylinder proportions can be obtained from equation (3) by writing the left-hand side of the equation in terms of the parameters $\bar{t}/R$ and N_x/R after use is made of equations (4) to eliminate D_x and to complete the stiffness ratio $\frac{E_r A_r}{E_x l}$ under the radical. Solution of $\bar{t}/R$ in terms of N_x/R results in the equation

$$\frac{\bar{t}}{R} = \sqrt{\frac{\frac{N_x}{E_t R}}{F_S}} \tag{5}$$

where F_S is given by

$$F_S = \left[\frac{2}{A_2}\left(\sqrt{A_1 A_2 + A_3{}^2} + A_3\right)\right] \frac{\frac{b}{t}\sqrt{\frac{E_r A_r}{E_x l}} \sin \phi(1 + \cos \phi)}{2\sqrt{6}\left(1 + \frac{E_r A_r}{E_x l} \frac{d_r}{d} \frac{E_t}{E_r}\right)^2} \tag{6}$$

The parameter F_S can be considered to be a shape factor for the problem at hand in much the same sense that ρ^2/A is the shape factor for columns. Large values of the shape factor result in low-mass structures; and, in a given design situation, the shape factor is made as large as possible for a given loading N_x/R by varying the geometry of the structure. Geometry variations must be restricted to those proportions which fail by general instability, the mode of failure for which equation (6) is formulated.

Equation (5) differs in two respects from similar equations that have been used in structural efficiency studies. In the first place, the buckle aspect ratio β does not normally appear in the shape factor; it is usually eliminated from the buckling equation before writing the buckling equation in terms of structural efficiency parameters. The other difference is concerned with the parameter b/t appearing in the expression for shape factor. This parameter would normally be eliminated by solving for b/t in terms of $\bar{t}/R$ and $\frac{N_x}{E_t R}$ from an equation for local buckling of the elements of the corrugated wall and by substituting the result in equations (5) and (6). Such a procedure would indicate that $\bar{t}/R$ varies as the three-fifths power of the structural index rather than the one-half power as indicated by equation (5). Hence, the one-half power variation is associated with structures in which b/t is held constant and the three-fifths power is associated with structures in which the local buckling stress of the corrugated wall is equated to the general-instability stress; in both types of study, all other parameters are held constant. The form indicated for equations (5) and (6) was chosen for convenience and for the increased generality afforded by the use of the equations over that of more conventional equations. This choice in no way affects the results calculated with the use of the equations, as will become evident in subsequent sections of this paper.

The ring cross section shown in figure 1(b) is employed in the calculations made herein. The section is representative of a large number of cross-sectional shapes, some of which are depicted in figure 2. All the sections may have lightening holes in the web of the ring.

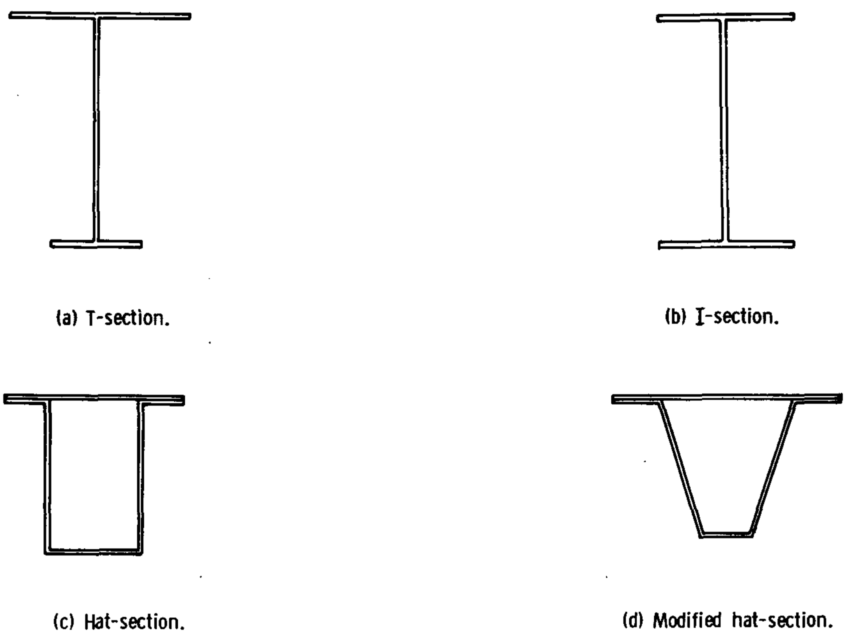

(a) T-section. (b) I-section.

(c) Hat-section. (d) Modified hat-section.

Figure 2.- Ring sections applicable to study.

With the ring cross section adopted, certain stiffness properties can be conveniently written in terms of other stiffness properties and pertinent ring and corrugation dimensions as follows:

$$\frac{E_r I_r}{D_x l} = 6\left(\frac{h}{f}\right)^2 \frac{E_r A_r}{E_x l} \frac{I_r}{A_r h^2} \tag{7a}$$

$$\frac{E_r A_r}{G_{xy} l} = \frac{8(1 + \mu)}{(1 + \cos \phi)^2} \frac{E_r A_r}{E_x l} \frac{E_t}{E_s} \tag{7b}$$

$$\frac{\bar{z}_r}{\rho_r} = \pm \frac{\frac{\bar{y}}{h} + \frac{1}{2}\frac{f}{h}}{\sqrt{\frac{I_r}{A_r h^2}}} \tag{7c}$$

where

$$\frac{\bar{y}}{h} = (1 - k)\gamma + \frac{1}{2}(1 - \gamma)$$

$$\frac{I_r}{A_r h^2} = \gamma \left[(1 - k)\left(1 - \frac{\bar{y}}{h}\right)^2 + k\left(\frac{\bar{y}}{h}\right)^2\right] + \frac{1 - \gamma}{3}\left[\left(\frac{\bar{y}}{h}\right)^3 + \left(1 - \frac{\bar{y}}{h}\right)^3\right]$$

$$\gamma = \frac{A_F}{A_r}$$

and k is the ratio of the area of the attachment flange of the ring to the area of both flanges. The positive sign in equation (7c) applies for external rings; the negative sign, for internal rings.

At this point, the geometric variables in the computation for shape factor are b/t, ϕ, k, γ, h/f, $\frac{G_r J_r}{D_x l}$, and $\frac{E_r A_r}{E_x l}$. The variables b/t and ϕ are associated with the shape of the corrugation; k and γ, with the shape of the reinforcing rings; h/f, $\frac{G_r J_r}{D_x l}$, and $\frac{E_r A_r}{E_x l}$, with the ratios of ring properties to corrugation properties. Obviously, the ratio b/t is determined by the local buckling stress of the corrugated wall; the ratio is made as large as possible without introducing local buckling of the corrugation. Constant values can be assigned to some of the other parameters with good accuracy. Others must be evaluated for each design. Each of the parameters is discussed more fully in the following section.

PARAMETRIC CONFIGURATION STUDIES OF INTERNALLY STIFFENED CYLINDERS

Inasmuch as equation (6) indicates that the shape factor is proportional to the ratio b/t, calculations of $\frac{F_S}{b/t}$ can be made which have general applicability instead of making computations for each value of b/t. This procedure is used herein. The ratio $\frac{G_r J_r}{D_x l}$ normally has little influence on the buckling strength of corrugated ring-stiffened cylinders. Hence this variable is taken into account in an approximate manner in all calculations. Calculations are first made with $\frac{G_r J_r}{D_x l} = 0$. The results of these calculations are then corrected, if necessary, after a ring shape has been selected.

Results of calculations to determine desirable values for certain variable parameters are given in figures 3 to 5. Figure 3 shows the variation of shape factor with the ratio $\frac{E_r A_r}{E_x l}$ for selected values of other parameters. The figure indicates that the ratio $\frac{E_r A_r}{E_x l}$ can be taken equal to 0.30 with little error. The results of similar calculations to determine the angle ϕ are shown in figure 4. Evidently, ϕ can be taken equal to 55° or 60° with little error. In all further calculations, ϕ is assumed to be equal to 60°.

The results of calculations to determine the effect of varying the parameter k are shown in figure 5. On the basis of these calculations, k is taken equal to 0.80 in further calculations for unsymmetrical rings. Selection of this value was tempered somewhat by the desire to provide sufficient ring material in the outstanding flange of the T-section ring $\left((1 - k)A_F\right)$ to support the web of the ring from lateral deformations. In selecting the 0.80 value, use was made of the study of reference 5, which provides an equation (eq. (14)) for determining the required flange material. Attainable values of the shape factor are compromised very little by the choice of the value 0.80.

The principal remaining parameters to be investigated are b/t, γ, and h/f. Each of these parameters will be individually chosen for each design situation. These parameters can be selected with the use of figure 6, where the shape factor $\frac{F_S}{b/t}$ is plotted against the ratio h/f for various values of the parameter γ. The calculations for figure 6 were made for $E_t = E_s = E_r$ and for $d = d_r$. Hence, figure 6 applies only to cylinders with rings of the same material as that of the corrugated wall and for loadings

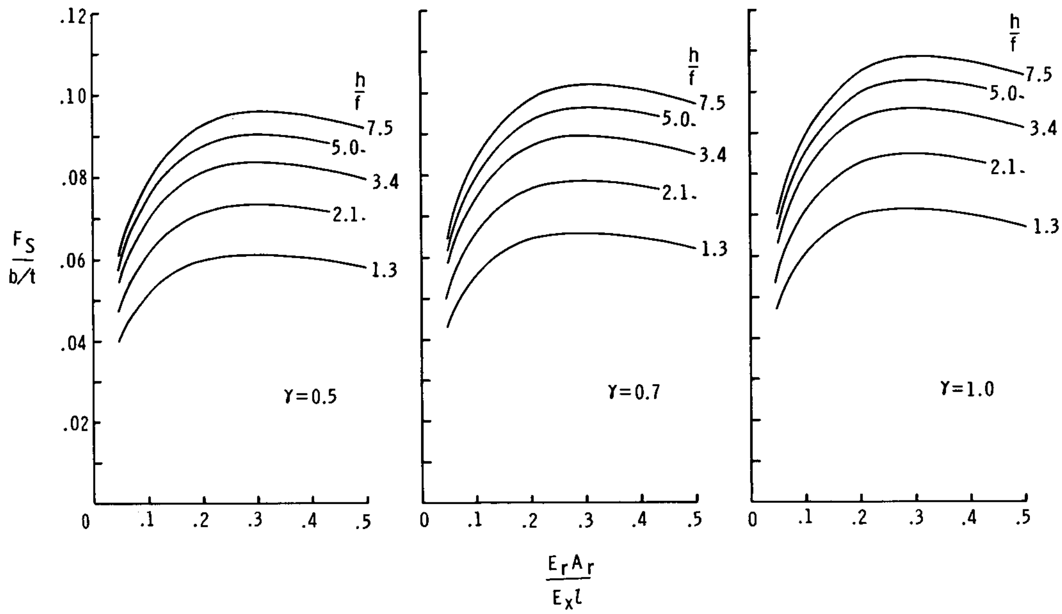

(a) k = 0.50.

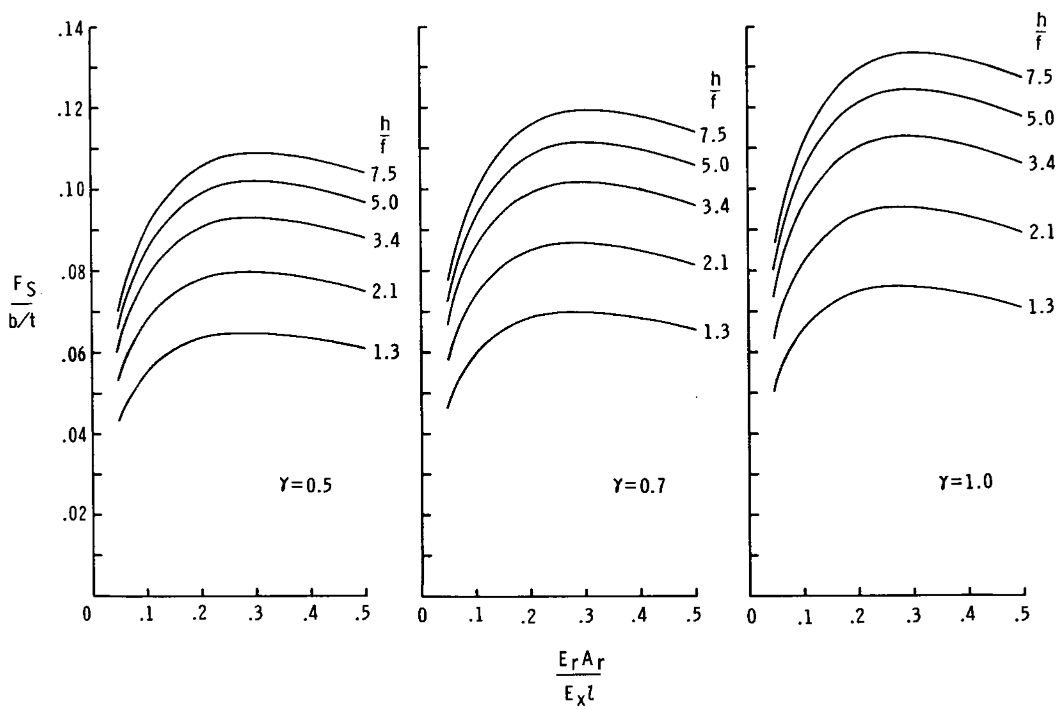

(b) k = 0.80.

Figure 3.- Calculations to determine desirable reinforcement ratio. $\Phi = 60^{0}$.

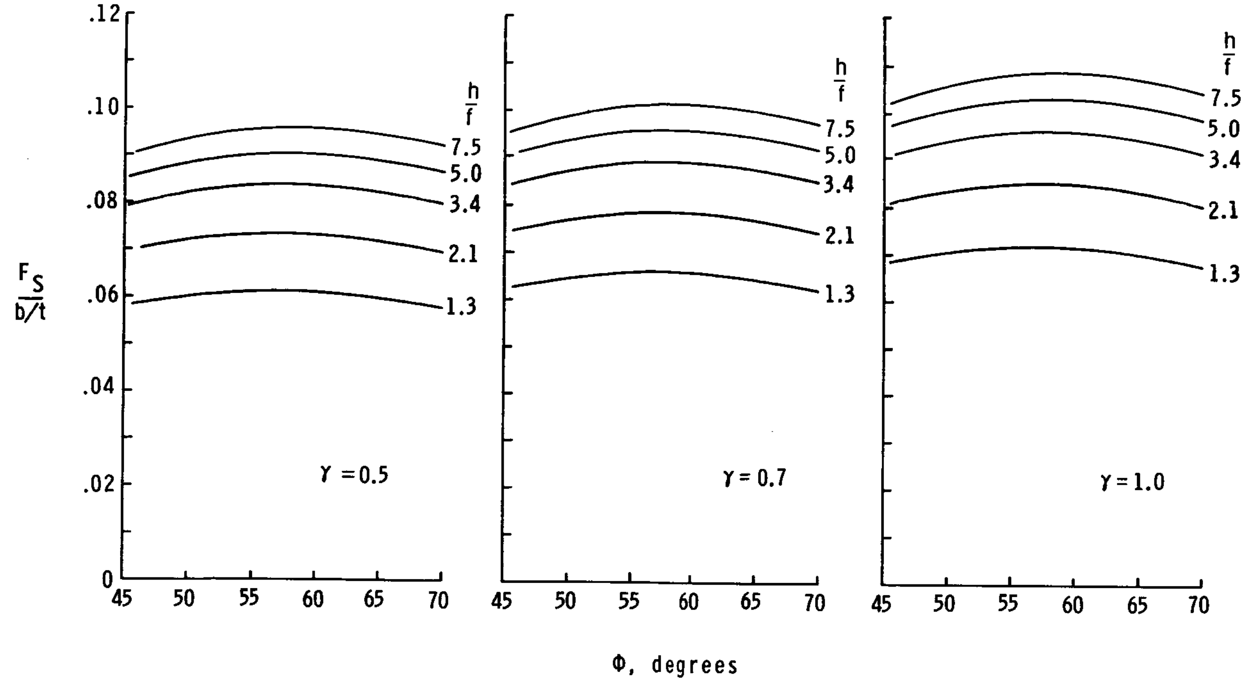

(a) k = 0.50.

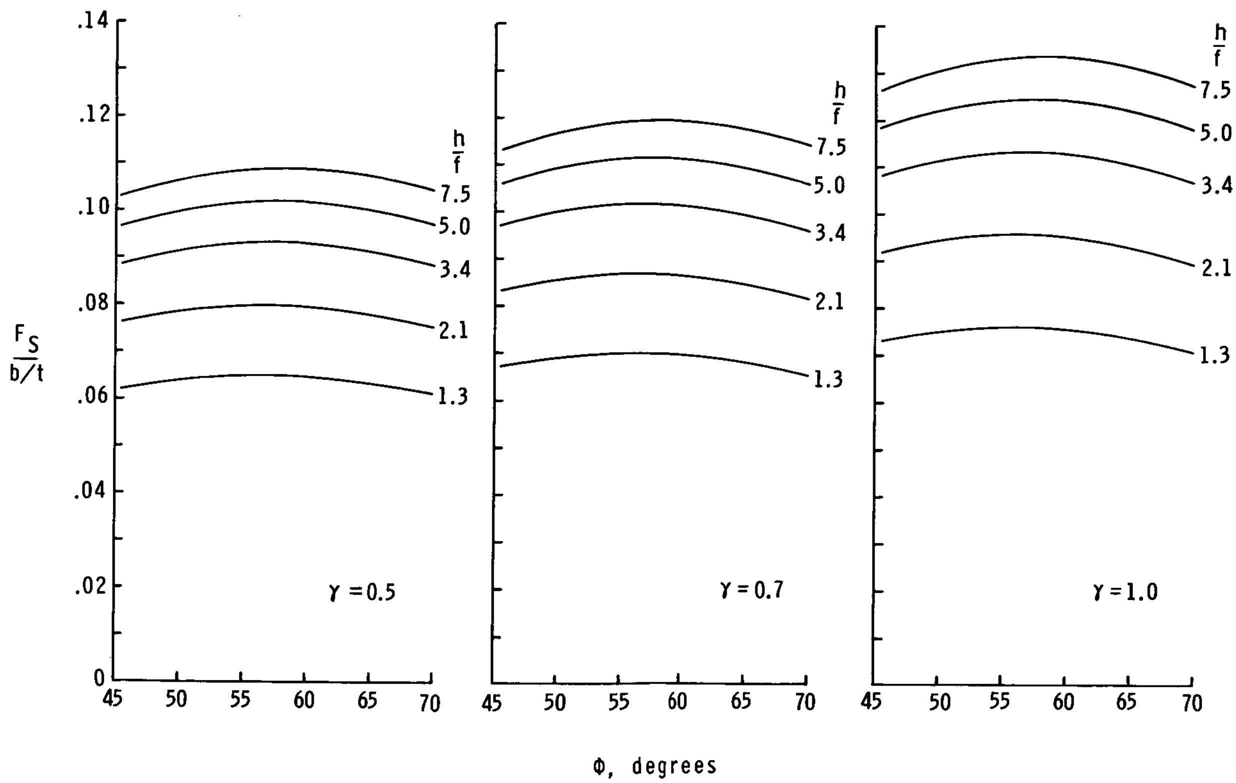

(b) k = 0.80.

Figure 4.- Calculations to determine desirable corrugation angle. $\frac{E_r A_r}{E_x l} = 0.30$.

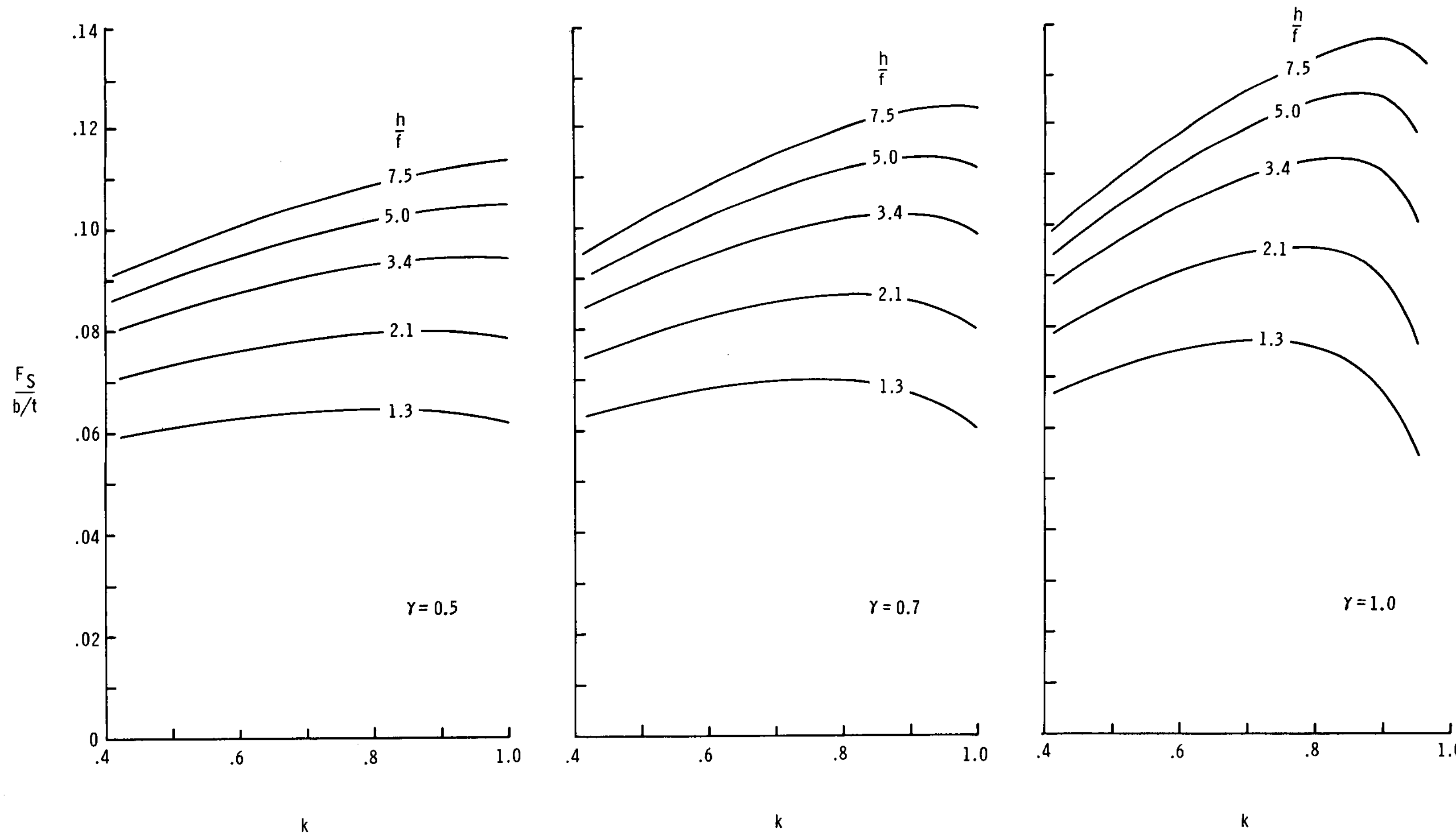

Figure 5.- Calculations to determine shape of stiffening ring. $\frac{E_r A_r}{E_x l} = 0.30$; $\Phi = 60^0$.

which cause stresses in the corrugated wall less than the proportional-limit stress of the corrugation material. Figure 6 can also be used for higher stresses and different materials with little error; however, in these cases, the shape factor read from this figure should be corrected by multiplying it by $\sqrt{\frac{d}{d_r}\frac{E_r}{E_t}}$ to obtain the corrected shape factor. The approximation involved in this correction can be seen by dividing both sides of equation (6) by the correction so that the stiffness parameter $\frac{E_r A_r}{E_x l}$ becomes a mass parameter $\frac{E_r A_r}{E_x l}\frac{d_r}{d}\frac{E_t}{E_r}$. The correction results from the fact that the ratio of the mass of the ring stiffeners to the mass of the corrugated wall, rather than the corresponding stiffness ratio, is approximately 0.30. The correction presumes conservatively that the shear stiffness of the corrugation is proportional to E_t rather than E_s, a tolerable assumption in most cases, particularly since the basic equation used to obtain the shear stiffness (eqs. (4)) is approximate. The correlation also presumes unconservatively that the factor $\frac{2}{A_2}\left(\sqrt{A_1 A_2 + A_3^2} + A_3\right)$ does not change with ring stiffness ratio although calculations indicate that the factor changes by small amounts.

It is seen from figure 6 that large values of γ and h/f produce large values of the shape factor. Large values of h/f and γ are associated with deep unstable rings. Hence, some restriction on these parameters is needed in order to insure the use of ring sections which perform their intended function, that is to stabilize the corrugated wall. The stability of individual rings can be improved by using fewer rings with heavier flanges and webs. Thus the rings should normally be spaced as far apart as possible without introducing failure between rings (panel instability). Reference 4 indicates that, for corrugated cylinders, this spacing is adequately given by the Euler column formula:

$$N_x = \frac{\pi^2 D_x}{l^2}$$

In terms of parameters of the problem at hand, the Euler equation can be written as

$$\sqrt{\frac{\sigma_{pan}}{E_t}} \leq \frac{2\pi \frac{E_r A_r}{E_x l}\frac{h}{t_W}(1 - \gamma)\frac{E_t}{E_r}}{\sqrt{6}\left(\frac{h}{f}\right)^2 \frac{b}{t}\sin\phi(1 + \cos\phi)}$$

or

$$\left(\frac{h}{f}\right)^2 \leq \frac{2\pi}{\sqrt{6}} \frac{\frac{E_r A_r}{E_x l} \frac{h}{t_W} (1 - \gamma) \frac{E_t}{E_r}}{\sqrt{\frac{\sigma_{pan}}{E_t} \frac{b}{t} \sin \phi(1 + \cos \phi)}} \tag{8}$$

where σ_{pan} is the axial stress in the corrugated wall at which panel instability would occur. Expressions (5) and (8) and figure 6 can be used to determine desirable proportions of ring-stiffened corrugated cylinders under axial compression. Their use is illustrated in the following section of the paper.

CONFIGURATION STUDIES OF RINGS OF INTERNALLY STIFFENED CYLINDERS

Several calculations, which make use of equations and graphs presented earlier, are discussed in this section of the paper in order to determine desirable ring geometries. Calculations are made for given values of the parameter h/t_W or, what amounts to the same thing, for given values of the local buckling stress of the rings. The parameter h/t_W is important because practical structures undergo lateral deformations during loading long before the applied load reaches the predicted buckling load of the structure. Such deformations load the ring in bending, shear, and compression or tension. Calculations indicate that rings should be deep for maximum efficiency; however, if rings are used with values of h/t_W that are too large, the deformations will buckle the rings and hence jeopardize their capacity to support the corrugated wall.

Information is lacking on how large h/t_W can be and still adequately support the corrugated wall, but the use of values larger than 80 should probably be avoided on the premise that unavoidable fabrication stresses may buckle the webs. If rings are formed by operations associated with large amounts of drawing of the ring material, smaller values than 80 may be desirable; fabrication stresses tend to be large in such components.

The method of ring design employed in the calculations discussed in this section of the paper depends upon the assumption that the modes of failure for panel instability and general instability differ appreciably; consequently, little or no interaction between the two modes evolves. This method is believed to be satisfactory for the corrugated cylinders investigated; it may not be satisfactory for some other types of construction. The buckling behavior of ring-stiffened corrugated cylinders is affected very little by prebuckling deformations (ref. 6). Moreover, the calculated modes for panel and general

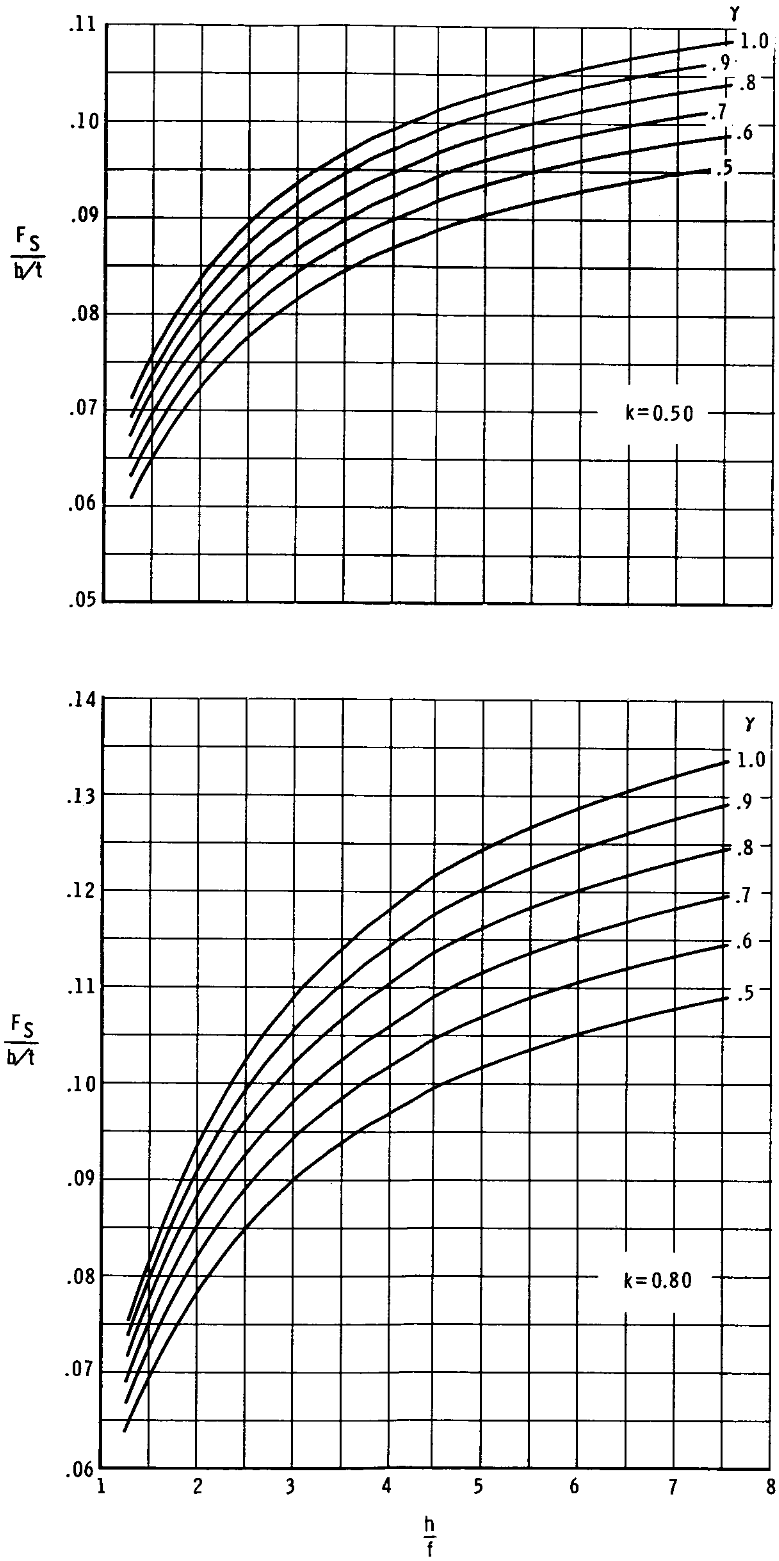

Figure 6.- Charts for determining desirable ring sections.

instability differ considerably for the corrugated cylinders investigated, and the method of ring design employed is expected to be satisfactory under such favorable conditions. On the other hand, it may not be satisfactory for structures for which the calculated modes for panel and general instability are not as dissimilar. The effect of prebuckling deformations in such structures is to effect a coalescence of the modes for general and panel instability (ref. 6).

Basic Calculation

As a basis for comparison with other calculated results, a calculation will be made for a cylinder fabricated from 7075-T6 aluminum alloy ($E = 10500$ ksi ($72.4\ GN/m^2$), $\mu = 0.32$, and $d = 0.101\ lbm/in^3$ ($2.80\ Mg/m^3$)). The following properties are assumed: $\phi = 60^o$, $k = 0.80$ (unsymmetrical, T-section rings), $\frac{h}{t_W} = 80$, and $\frac{E_r A_r}{E_x l} = 0.30$. The cylinder is proportioned so that local buckling, panel instability, and general instability occur simultaneously $\left(\sigma_{loc} = \sigma_{pan} = \sigma_{gen}\right)$.

From equation (8) (by assuming elastic behavior)

$$\left(\frac{h}{f}\right)^2 = 24.7(1 - \gamma)$$

because the product $\frac{b}{t}\sqrt{\frac{\sigma_{pan}}{E_t}}$ is a constant (≈1.92). By assuming various values of γ (0.5, 0.6, 0.7, etc.), values of $\frac{F_S}{b/t}$ can be read from figure 6 after consistent values of h/f have been computed. By plotting $\frac{F_S}{b/t}$ against γ or h/f, the maximum value of $\frac{F_S}{b/t}$ can be obtained. This value is found to be $\frac{F_S}{b/t} = 0.0955$; consistent values for γ and h/f are $\gamma = 0.64$ and $\frac{h}{f} = 2.98$.

For a given value of b/t (stress), values of N_x/R and $\bar{t}/R$ can be computed from equation (5). For instance, for $\frac{b}{t} = 30$, $\sigma_{pan} = 43.0$ ksi ($296\ MN/m^2$), and $\epsilon = 0.0041$,

$$\frac{\bar{t}}{R} = \frac{\bar{t}_x}{R}\left(1 + \frac{E_r A_r}{E_x l}\right) = \frac{N_x}{ER\epsilon}\left(1 + \frac{E_r A_r}{E_x l}\right) = \sqrt{\frac{N_x/ER}{F_S}}$$

Hence

$$\frac{N_x}{R} = \frac{E\epsilon^2}{F_S\left(1 + \frac{E_r A_r}{E_x l}\right)^2} = 0.0364 \text{ ksi } (251 \text{ kN/m}^2)$$

$$\frac{\bar{t}_x}{R} = \frac{N_x}{R}\frac{1}{\sigma} = 0.000847$$

$$\frac{\bar{t}}{R} = 1.3\frac{\bar{t}_x}{R} = 0.00110$$

Values of the shape factor F_S computed as in this example are plotted in figure 7 for various values of h/t_W. It will be noted that large values of the shape factor F_S are associated with large values of h/t_W; hence, in any practical application, a limitation must be assigned to this parameter, as previously discussed.

Other Calculations

I-section ring.- A calculation similar to the basic calculation but with $k = 0.50$ instead of $k = 0.80$ yields for $\frac{h}{t_W} = 80$ and $\frac{b}{t} = 30$

$$F_S = 2.55$$

$$\gamma = 0.65$$

$$\frac{h}{f} = 2.94$$

$$\frac{N_x}{R} = 0.0408 \text{ ksi } (281 \text{ kN/m}^2)$$

This result is represented in figure 7 as the circular symbol and should be compared with the $\frac{h}{t_W} = 80$ curve. As discussed previously, I-section rings ($k = 0.50$) are seen to be less efficient than T-section rings ($k = 0.80$).

Magnesium rings.- Because the principal contribution of rings is stiffness, a calculation is made with the use of magnesium rings ($E = 6500$ ksi (44.8 GN/m^2) and $d = 0.064 \text{ lbm/in}^3$ (1.77 Mg/m^3)). In order to obtain a magnesium ring which is equivalent to the aluminum ring $\frac{h}{t_W} = 80$ from a local buckling point of view, the loads for buckling of equal-mass aluminum and magnesium rings are equated. Such a consideration leads to the result that the equivalent magnesium ring has a depth-thickness ratio of

$$\frac{h}{t_W} = 80\sqrt{\frac{d_{Al}}{d_{Mg}}\frac{E_{Mg}}{E_{Al}}} \approx 80$$

and from equation (8)

$$\left(\frac{h}{f}\right)^2 = 39.0(1 - \gamma)$$

The calculation for shape factor is made as before except a correction to the factor as read from figure 6, as discussed previously, is required. The correction in this case is $\sqrt{\frac{d_{Al}}{d_{Mg}}\frac{E_{Mg}}{E_{Al}}}$. Hence, for $\frac{b}{t} = 30$,

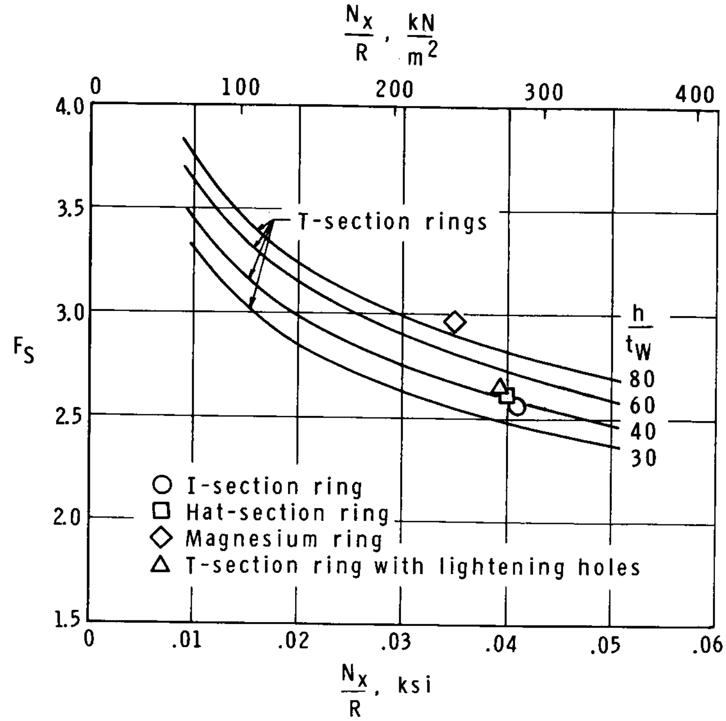

Figure 7.- Shape factor for cylinders with different types of rings.

$$F_S = 3.01$$

$$\gamma = 0.66$$

$$\frac{h}{f} = 3.63$$

$$\frac{N_x}{R} = 0.0347 \text{ ksi } (239 \text{ kN/m}^2)$$

This result is plotted in figure 7 as the diamond symbol and should be compared with the $\frac{h}{t_W} = 80$ curve. There is evidently a small theoretical advantage in using magnesium rings in place of aluminum rings.

Hat-section rings.- Rings such as those shown in figures 2(c) and 2(d) can be handled in much the same manner as the T-section rings. After F_S and N_x/R are computed in the usual manner, ring area is computed and distributed in the form of a hat-section ring. The parameter $\frac{G_r J_r}{D_x l}$ is then computed and a corrected shape factor that includes the influence of a finite ring torsional stiffness is computed from equation (6). The loading index is also corrected accordingly.

Thus, for $\frac{h}{t_W} = 30$ $\left(\text{two webs of } \frac{h}{t_W} = 60\right)$

$$\left(\frac{h}{f}\right)^2 = 9.26(1 - \gamma)$$

and for $\frac{G_r J_r}{D_x l} = 0$ and $\frac{b}{t} = 30$

$$F_S = 2.42$$

$$\frac{h}{f} = 1.99$$

$$\gamma = 0.57$$

$$\frac{N_x}{R} = 0.0431 \text{ ksi } (297 \text{ kN/m}^2)$$

The stiffness ratio $\frac{G_r J_r}{D_x l}$ for a ring section such as shown in figure 2(c) is computed as $\frac{G_r J_r}{D_x l} = 0.22$. The corrected shape factor is computed from equation (6) with the use of the computed values of $\frac{h}{f} = 1.99$ and $\gamma = 0.57$ and is as follows:

$$\left(F_S\right)_{corr} = 2.61$$

The corrected value of the loading index is

$$\left(\frac{N_x}{R}\right)_{corr} = 0.0400 \text{ ksi } (276 \text{ kN/m}^2)$$

This result, given in figure 7 as the square symbol, should be compared with other results for $\frac{h}{t_W} = 60$ (rings with an equivalent local buckling stress). It is noted that a small loss in calculated efficiency was obtained by shaping the rings into hat sections.

Rings with lightening holes.- Rings having webs with lightening holes will be compared with those without holes. In order to facilitate the comparison, a calculation is made for a web with $\frac{h}{t_W} = 40$ and with lightening holes having a diameter equal to $\frac{3}{4}h$ and a spacing equal to $\frac{7}{8}h$. Such a web has about the same mass as a solid web of the same depth with $\frac{h}{t_W} = 80$. For computational purposes, it is assumed that the web with holes contributes nothing toward the area and moment of inertia of the ring ($\gamma = 1.0$).

The calculation is made with the use of figure 6; several values of h/f are assumed and corresponding values of F_S are obtained from the figure for $\gamma = 1.0$. These values are corrected by multiplying them by the square root of the ring stiffness ratio divided by the ring mass ratio for reasons discussed previously for highly stressed (plastic) cylinders and cylinders with rings of a different material than the corrugated wall. A relationship between the stiffness ratio and the mass ratio is needed in order to obtain the correction. The relationship can be obtained from the Euler column equation in much the same manner that equation (8) was obtained. Thus, the mass ratio, which was taken as 0.30, can be written as

$$0.30 = \frac{E_r A_r}{E_x l} + \frac{1}{2}\,\frac{\sqrt{6}\left(\frac{h}{f}\right)^2 \frac{b}{t}\sqrt{\epsilon}\,(1 + \cos\phi)\sin\phi}{2\pi\frac{h}{t_W}}$$

where the first term on the right-hand side of the equality sign is the stiffness ratio and the factor 1/2 in front of the second term indicates that only one-half of the mass of the webs remain after lightening holes are cut. Thus, for $\frac{h}{t_W} = 40$, $\frac{b}{t} = 30$, $\epsilon = 0.0041$, and $\phi = 60^\circ$,

$$\frac{E_r A_r}{E_x l} = 0.30 - 0.0121\left(\frac{h}{f}\right)^2$$

When the corrected values of F_S are computed and plotted against h/f, the maximum value of F_S can be ascertained. Thus,

$$F_S = 2.64$$

$$\frac{h}{f} = 2.4$$

$$\frac{N_x}{R} = 0.0395 \text{ ksi } (272 \text{ kN/m}^2)$$

This result is given in figure 7 as the triangular symbol and should be compared with the curves for $\frac{h}{t_W} = 80$ and $\frac{h}{t_W} = 40$. Because the webs with lightening holes fall between the curves for solid webs of $\frac{h}{t_W} = 40$ and $\frac{h}{t_W} = 80$, some improvement in efficiency is indicated by the use of lightening holes $\left(\text{compare with } \frac{h}{t_W} = 40 \text{ curve}\right)$; however, not as much improvement is indicated as would be achieved by thinning the web to obtain an equivalent-mass solid web $\left(\text{compare with } \frac{h}{t_W} = 80 \text{ curve}\right)$. Thus, the use of lightening holes does not appear to offer very substantial gains in efficiency, although a better calculation in which the webs with holes are assumed to carry some load would undoubtedly show the webs as somewhat more competitive with solid webs.

CONFIGURATION STUDY OF EXTERNALLY STIFFENED CYLINDERS

The buckling behavior of corrugated cylinders with external stiffening is considerably different from that of internally stiffened cylinders. Calculations indicate that externally stiffened cylinders buckle into an axisymmetric mode for a wide range of ring configurations. Hence the structural efficiency of externally stiffened cylinders is reasonably independent of ring shape, and shallow rings are just as efficient as deeper less stable rings as long as the depth is sufficient to insure buckling in the axisymmetric mode. In this regard, care must be taken to use rings deep enough to satisfy the inequality

$$\frac{E_r I_r}{D_x l} > \frac{E_r A_r}{E_x l}$$

so that buckling in a mode having a very large buckle aspect ratio is not critical. Even rather shallow rings satisfy this criterion, and rings with a depth of 1.3 times the corrugation depth (the shallowest rings studied) were found to be adequate to force failure into the axisymmetric mode. Moreover, symmetrical (I-section) rings were found to be just as efficient as unsymmetrical (T-section) rings, and no advantage was found in spacing the rings so that panel-instability and general-instability failures were "balanced."

Manipulation of equation (2) or equation (3) indicates that for the axisymmetric mode

$$\frac{N_x R}{\sqrt{D_x \frac{E_r A_r}{l}}} = 2.0 \tag{9}$$

Equation (6) then yields

$$\left.\begin{aligned}\phi &= 60^{\circ} \\ \frac{E_r A_r}{E_x l} &= \frac{1}{3}\end{aligned}\right\} \tag{10}$$

and

$$F_S = 0.172 \frac{b}{t} \tag{11}$$

The structural efficiency of externally stiffened cylinders is compared with that of internally stiffened cylinders and with honeycomb sandwich cylinders in the following section of the paper.

FURTHER REMARKS

In the calculations presented, desirable proportions of ring-stiffened corrugated cylinders were obtained. The calculations neglect certain wall stiffness contributions to the buckling strength of cylinders (eq. (1)) because the contributions are known to be relatively small. If experimental results were available, the buckling loads calculated by neglecting the stiffness contributions might be expected to agree reasonably well with the experiments. References 7 and 8 used stiffnesses and buckling theories comparable to those used herein and obtained reasonably good agreement between calculation and test for somewhat different configurations than those considered herein. This agreement masks, to some degree, mutually compensating errors due to neglect of the wall stiffnesses, initial imperfections, and so forth. The use of more accurate expressions for stiffnesses in calculating buckling loads results in the prediction of too high buckling loads (refs. 4 and 9) – loads which must be modified by some appropriate means to correlate with experiment. So far, an appropriate means of correlation has not been found but the neglect of those stiffnesses neglected herein seems to conveniently accomplish this end.

It was stated previously that the ring-stiffened corrugated cylinder is rather attractive from a low-mass, high-strength point of view. The calculations made herein can be used to investigate the general validity of this statement. A comparison with honeycomb sandwich cylinders is made in figure 8. The curve for corrugated cylinders with internal stiffening represents those calculations given earlier for $\frac{h}{t_W} = 80$ and the curve for external stiffening was obtained with the use of equations (5) and (11). Both curves have the three-fifths power variation in the elastic range, as discussed earlier. The curve for honeycomb sandwich cylinders was taken directly from figure 14 of reference 10. The reference curve applies to adhesively bonded sandwich cylinders with reasonably heavy cores ($\delta = 0.03$). The calculations made to obtain the reference curve were partly substantiated by the tests of reference 11. Thus, the curve is believed to be representative of good quality sandwich construction.

The comparison shown in figure 8 indicates that the corrugated cylinders are rather attractive from a low-mass, high-strength point of view, with the externally stiffened cylinders appearing somewhat more attractive and the internally stiffened cylinders appearing somewhat less attractive than the honeycomb sandwich cylinders. However, the corrugated construction is less expensive and more reliable than the honeycomb sandwich construction to which it is compared and evidently should be considered in designs where these factors as well as low mass are important design considerations. The externally stiffened corrugated construction should evidently be considered in designs where the external rings are not a liability.

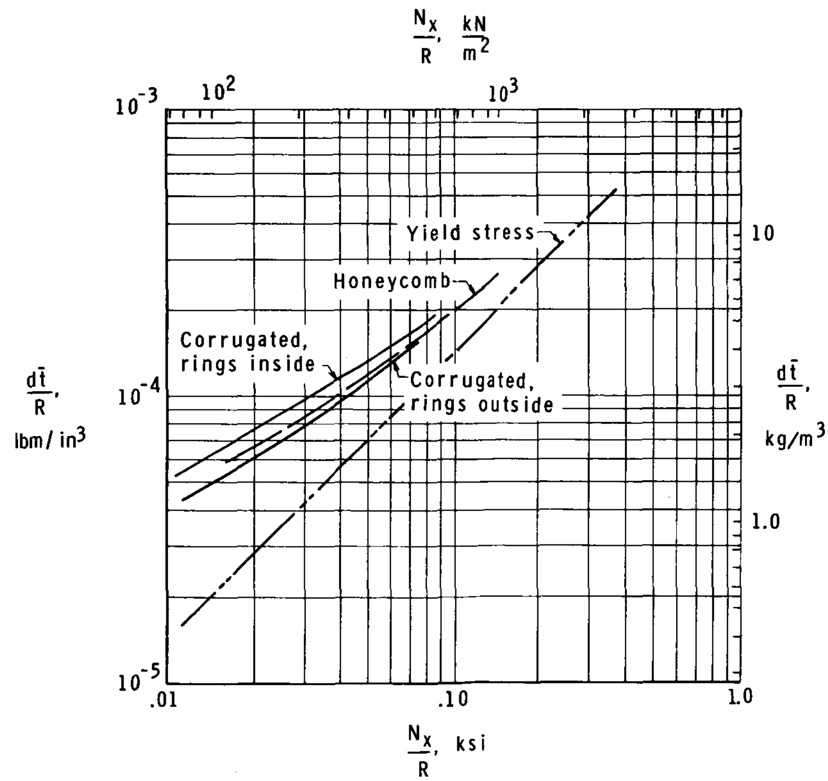

Figure 8.- Comparison of ring-stiffened corrugated cylinders with honeycomb sandwich cylinders.

Although calculated configurations for low-mass, high-strength structures are normally obtained by equating possible modes of failure, practical applications of such calculations would undoubtedly indicate that more reliable configurations would result if certain modes of failure had small margins against failure. The charts of figure 6 are well adapted for use in determining configurations with margins against failure in certain modes. For instance, for the internally stiffened cylinder considered in the basic calculation given earlier, a calculation will be made in which the stress at general instability is taken as 90 percent of the stress for panel instability and local buckling.

As before, equation (8) gives

$$\left(\frac{h}{f}\right)^2 = 24.7(1 - \gamma)$$

and maximum efficiency is again attained when $\frac{F_S}{b/t} = 0.0955$, $\gamma = 0.64$, and $\frac{h}{f} = 2.98$. For $\frac{b}{t} = 30$ $\left(F_S = 2.86\right)$, $\epsilon_{loc} = \epsilon_{pan} = 0.0041$ and $\epsilon_{gen} = 0.90(0.0041) = 0.00369$. Hence, with the use of the results of the basic calculation given previously,

$$\frac{N_x}{R} = (0.90)^2(0.0364) = 0.0294 \text{ ksi} \quad (203 \text{ kN/m}^2)$$

and

$$\frac{\bar{t}}{R} = (0.90)(0.00110) = 0.000990$$

This result would plot about 2 percent above the curve for internally stiffened corrugated cylinders in figure 8. Hence, for a calculated margin of 10 percent against failure in the local and panel instability modes, only a 2-percent penalty in mass results. It should be noted that a gain in efficiency, rather than a loss, may actually result; the "unbalanced" design is less susceptible to interaction between failure modes than the "balanced" design and hence is more likely to develop calculated strength.

CONCLUDING REMARKS

A study to determine desirable geometric parameters for axially compressed ring-stiffened corrugated cylinders is presented and discussed. The study revealed the following desirable characteristics for cylinders with rings attached to the inside surface of the cylinder wall: (1) The corrugated skin should have a corrugation angle ϕ of about 60° and should have elements with width-thickness ratios b/t determined by the stress level. (2) Rings with approximately 80 percent of the total flange area in the attachment flange (k = 0.80) are superior to symmetrical rings (k = 0.50). (3) Ring mass should be approximately 30 percent of the mass of the corrugated wall and the rings should be spaced as far apart as possible without introducing panel instability. (4) Rings should be deep for maximum efficiency; their depth is limited by factors such as fabrication stresses and initial imperfections which tend to destroy the stiffness properties of deep, thin-gage rings. (5) Little advantage, if any, was found (a) in substituting magnesium rings for aluminum rings on an aluminum cylinder, (b) in substituting closed hat-section rings for T-section rings, and (c) in substituting rings with webs having lightening holes for rings with solid webs.

For cylinders with rings attached to the outside surface of the cylinder wall, a corrugation with $\phi = 60^{\circ}$ and with b/t determined by the stress level was again found to be attractive. However, ring shape and ring spacing were found to be relatively unimportant and ring mass was found to be 1/3 of the mass of the corrugated wall.

Ring-stiffened corrugated cylinders were found to be attractive from a low-mass, high-strength point of view; the externally stiffened cylinders were somewhat more attractive and the internally stiffened cylinders were somewhat less attractive than honeycomb sandwich cylinders from this viewpoint. However, the corrugated cylinders are less expensive and more reliable than honeycomb sandwich cylinders.

Langley Research Center,
National Aeronautics and Space Administration,
Langley Station, Hampton, Va., January 24, 1967,
124-11-06-04-23.

APPENDIX

CONVERSION OF U.S. CUSTOMARY UNITS TO SI UNITS

The International System of Units (SI) was adopted by the Eleventh General Conference on Weights and Measures, Paris, October 1960, in Resolution 12 (ref. 2). Conversion factors for the units used in this report are given in the following table:

Physical quantity	U.S. Customary Unit	Conversion factor (*)	SI Unit
Length	in.	0.0254	meters (m)
Stress, modulus . . .	ksi	6.895×10^6	newtons/meter^2 (N/m^2)
Density.	lbm/in^3	27.68×10^3	kilograms/meter^3 (kg/m^3)

*Multiply value given in U.S. Customary Units by conversion factor to obtain equivalent value in SI Units.

Prefixes to indicate multiple of units are as follows:

Prefix	Multiple
giga (G)	10^9
mega (M)	10^6
kilo (k)	10^3

REFERENCES

1. Sterett, James B., Jr.: Shell Stability Problems in the Design of Large Space Vehicle Boosters. Collected Papers on Instability of Shell Structures – 1962, NASA TN D-1510, 1962, pp. 57-66.
2. Mechtly, E. A.: The International System of Units – Physical Constants and Conversion Factors. NASA SP-7012, 1964.
3. Block, David L.; Card, Michael F.; and Mikulas, Martin M., Jr.: Buckling of Eccentrically Stiffened Orthotropic Cylinders. NASA TN D-2960, 1965.
4. Peterson, James P.; and Anderson, James Kent: Bending Tests of Large-Diameter Ring-Stiffened Corrugated Cylinders. NASA TN D-3336, 1966.
5. Anderson, Melvin S.: Compressive Crippling of Structural Sections. NACA TN 3553, 1956.
6. Block, David L.: Influence of Ring Stiffeners and Prebuckling Deformations on the Buckling of Eccentrically Stiffened Orthotropic Cylinders. Ph.D. Thesis, Virginia Polytech. Inst., 1966.
7. Hedgepeth, John M.; and Hall, David B.: Stability of Stiffened Cylinders. AIAA J., vol. 3, no. 12, Dec. 1965, pp. 2275-2286.
8. Dickson, John N.; and Brolliar, Richard H.: The General Instability of Ring-Stiffened Corrugated Cylinders Under Axial Compression. NASA TN D-3089, 1966.
9. Anderson, James Kent: Bending Tests of Two Large-Diameter Corrugated Cylinders With Eccentric Ring Stiffeners. NASA TN D-3702, 1966.
10. Peterson, James P.: Weight-Strength Studies of Structures Representative of Fuselage Construction. NACA TN 4114, 1957.
11. Peterson, James P.; and Anderson, James Kent: Structural Behavior and Buckling Strength of Honeycomb Sandwich Cylinders Subjected to Bending. NASA TN D-2926, 1965.

NASA-Langley, 1967 —— 32 L-5197